Chemical Engineering Journal 152 (2009) 428–433

Contents lists available at ScienceDirect

Chemical Engineering Journal

journal homepage: www.elsevier.com/locate/cej

Dynamic experiments and model of hydrogen and deuterium separation with micropore molecular sieve Y at 77 K

Chu Xiao-Zhong[a,*], Zhao Yi-Jiang[a], Kan Yu-He[a], Zhang Wei-Guang[a], Zhou Shou-Yong[a], Zhou Ya-Ping[b], Zhou Li[b]

[a] Jiangsu Key Laboratory for Chemistry of Low-Dimensional Materials, Department of Chemistry, Huaiyin Teachers College, 111, Changjiang Road, Huai'an, 223300, PR China
[b] High Pressure Adsorption Laboratory, State Key Laboratory of Chemical Engineering, Tianjin University, Tianjin, 300072, PR China

ARTICLE INFO

Article history:
Received 18 January 2009
Received in revised form 20 April 2009
Accepted 30 April 2009

Keywords:
Molecular sieve
Hydrogen isotope
Adsorption
Separation
Model

ABSTRACT

The equilibrium and kinetic adsorption data of H_2 and D_2 on the micropore molecular sieve Y were collected at 77 K with the volumetric setup, and adsorption rate constants of deuterium evaluated from kinetic adsorption isotherms are larger than that of hydrogen at low pressure. In order to further study the influence factor of hydrogen isotope separation, the breakthrough curves of H_2 and D_2 mixture on this adsorbent were measured with the single column adsorption apparatus. Effects of different flow rate and pressure on separation efficiency were investigated, and up to 1.52 of the separation factor is obtained at the total gas pressure of 0.4 MPa and flow rate of 129.79 cm^3/min with the adsorption bed length of 1.0 m. However, the ratios of the adsorbed amount of deuterium over hydrogen are only 1.18 and 1.17 at 0.0139 and 0.0175 MPa, respectively. Based on the difference between equilibrium adsorption and dynamic adsorption in the column, the key factor of separating H_2 and D_2 mixture depends on their dynamic difference. Lastly, a model for the fixed adsorption bed was built to simulate the concentration distribution of H_2 and D_2, and the simulation results agree well with experimental results.

1. Introduction

The heavy isotope of hydrogen, deuterium, is an important material in nuclear industry. It also has important application in medical cure and as a tracer. Moreover, deuterium and tritium is consumed less than 10% in the nuclear fusion reactor, thus, they must be recovered and separated in order to reuse them [1]. Therefore, searching for a low-cost separation method is critical for the application of deuterium. However, the separation between hydrogen isotopes is difficult because of the similarity of isotope properties. Industrialized methods, such as cryogenic distillation, laser, and thermal diffusion, are highly energy consumptive [2–4]. Nevertheless, the separation cost is usually low if the separation is based on the difference of components in adsorption [5–7], and the adsorbent is a decisive factor of feasibility and separation cost. According to the research results of equilibrium adsorption before, the highest adsorption capacity for H_2 and D_2 is observed on the molecular sieve Y that pore size is approximate 0.7 nm [8], therefore, this adsorbent was selected to study equilibrium and kinetic adsorption behaviors of H_2 and D_2 with a volumetric setup and a single column adsorption apparatus. Furthermore, a model was built for simulation of the concentration distribution for binary hydrogen isotopes in the column.

2. Experimental

2.1. Materials and instruments

The molecular sieve Y was provided by the Molecular Sieve Factory, Nankai University, China. The adsorbent was grinded and sifted to particle sizes of 0.4–0.5 mm. The pore size is approximate 0.7 nm and other major parameters of Y are listed in Table 1. Hydrogen of purity above 99.995% was provided by Liu-Fang High-Tech Co., China. Deuterium of purity above 99.9% was provided by Haipu Gas Industry Co., Beijing. Mass flow controller is of precision 1.5% that was provided by Shengye Technical and Development Co., Beijing. Reconstructed gas chromatography 6890 was provided by Lunan Chemical Instrument Co., China [9]. AS-3100Plus specific surface area and pore size analyzer was provided by Beckman Coulter, USA. KK8 gas compressor was provided by DURR TECKNIK, German. Pressure transducer and molecular pump were provided by Pfeifer Vacuum, and the pressure sensor is of precision 0.2%. Rotary pump was provided by Vacuum Pump Co., Wuxi. The concentration of feed gas was analyzed with the gas chromatography, and the volumetric ratio of H_2, D_2 and He in the mixture is 3.49:4.36:92.15.

* Corresponding author. Tel.: +86 0517 83050008; fax: +86 0517 83525369.
E-mail address: chuxiaozhong@hytc.edu.cn (X.-Z. Chu).

1385-8947/$ – see front matter © 2009 Elsevier B.V. All rights reserved.
doi:10.1016/j.cej.2009.04.068

Nomenclature

C_i	sorbate concentration in fluid phase (mol/m^3)
ε	voidage of the column
ε_p	voidage of the adsorbent
μ	superficial velocity (m/s)
L	adsorbent bed length (m)
z	distance measured from column inlet (m)
t	time (s)
ρ	density of adsorbent in bed (kg/m^3)
ρ_s	apparent density (kg/m^3)
ρ_g	gas density (kg/m^3)
K_i	overall mass transfer coefficient (m/s)
q_i	adsorption amount (kg/mol)
q_t	adsorption amount at the time t (mol/kg)
q_{si}	saturation adsorption amount (mol/kg)
q_e	equilibrium adsorption amount (mol/kg)
b_i	affinity of adsorbate to adsorbent
p_i	partial pressure (MPa)
σ	specific surface area per unit volume adsorbent (m^2/m^3)
A	specific surface area (m^2/g)
μ	viscosity of the fluid (Pa s)
d	internal diameter of the column (m)
d_p	adsorbent pellet diameter (m)
R_p	pore radius of the adsorbent (m)
D_{ei}	effective axial diffusion coefficient (m^2/s)
D_i	intraparticle diffusivity (m^2/s)
D_{ai}	axial diffusion coefficient in the column
D_m	molecular diffusivity (m^2/s)
D_k	Knudsen diffusion coefficient (m^2/s)
D_s	surface diffusivity (m^2/s)
M	mole mass (kg/mol)
T	temperature (K)
Σv	molecular diffusion volume (cm^3/mol)
τ	tortuosity factor of the adsorbent
Re	Reynold number
Sc	Schmidt number
k	adsorption rate constant

Subscript

i	component i

2.2. Experimental apparatus and operation procedures

It is impossible to use microbalance at 77 K, therefore, the equilibrium and kinetic adsorption data were collected with a volumetric setup in Fig. 1 that was commonly used for the adsorption of nitrogen at 77 K to evaluate the BET surface area of adsorbents.

Table 1
Experimental condition and parameters in simulation.

Parameters	Value	Parameters	Value
L (m)	1	ρ_g (kg/m^3)	0.630
d (m)	0.005	d_p (m)	4.0×10^{-4}
ε	0.42	p (MPa)	2.0–8.0
κ (H_2)	1.74[1]	κ (D_2)	1.50[1]
ρ (kg/m^3)	624.20	A (m^2/g)	367.04
ρ_s (kg/m^3)	1300.43	u (m/s)	0.05–0.2
$(\sum v)_{H_2}$ (cm^3/mol)	7.07	σ (m^2/m^3)	2.29×10^8
$(\sum v)_{D_2}$ (cm^3/mol)	6.70	D_s(H_2) (m^2/s)	2.5×10^{-9}[2]
$(\sum v)_{He}$ (cm^3/mol)	2.88	D_s(D_2) (m^2/s)	2.0×10^{-9}[2]

* Data of (1) and (2) are cited from Refs. [19,17], respectively.

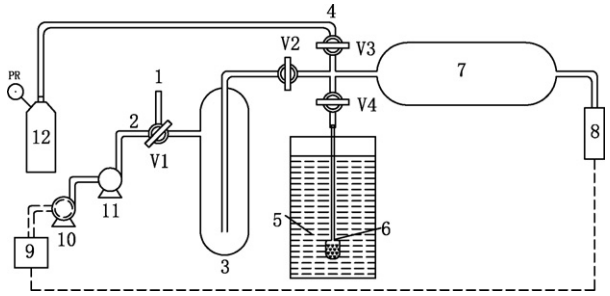

Fig. 1. Schematic apparatus for adsorption experiments: (1) vent, (2) vacuum exit, (3) buffer bottle, (4) feed gas inlet, (5) liquid tank, (6) adsorption cell, (7) reference cell, (8) pressure transmitter, (9) on-line data recorder system, (10) molecular pump, and (11) vacuum pump V1 three-way vacuum valve V2, V3, V4 two-way vacuum valve.

The variation of pressure with time, $p(t)$, was detected by a pressure transmitter and recorded in a computer via Labcards. The adsorption cell is initially in vacuum (0.01 Pa) for both equilibrium and kinetic adsorption measurements. However, the pressure in the adsorption cell was increased stepwise until 0.12 MPa for collecting equilibrium isotherms, while only the initial pressure of the reference cell was controlled in kinetic experiments and five levels of initial pressure were measured. The temperature of the reference cell was kept constant within ±0.2 K, and the temperature of the adsorption cell was kept constant at 77 K with liquid nitrogen of constant level. The absolute relative error calculated for the adsorption amount was within 2.0 [10].

As shown in Fig. 2, hydrogen isotopes separation by cryogenic adsorption was conducted by a single column adsorption apparatus. First, the adsorbent was regenerated at 150 °C by evacuation for 24 h before adsorption measurements, and then was filled in the adsorption bed that was soaked in liquid nitrogen cylinder. Second, the overall apparatus was adjusted to the desired flow rate and pressure with carrier gas He after its evacuation. Thirdly, the feed gas entered the column via a cold trap at 77 K, and then passed through the column at the given flow rate and pressure, and simultaneously, the concentration of the hydrogen isotopes was measured at the outlet of the column with gas chromatography. Effects of different flow rate and pressure on separation efficiency were investigated in the experiments.

3. Model

3.1. Formulation of the model

To develop a generalized model for the adsorption bed, following assumptions for H_2 and D_2 separation process on the molecular sieve Y were given [11–14]:

- Ideal gas is postulated for H_2 and D_2.
- Plug flow is postulated for the gas passing through the adsorbent bed.
- The pressure over the adsorbent bed is constant.
- The temperature of the adsorbent bed is constant.

Due to low H_2 and D_2 concentration in the feed gas, low flow rate and large ratio of length to diameter of the column ($L/d = 20$), assumptions proposed above are reasonable.

On the basis of mass balance for the H_2 or D_2 component i in the adsorption bed, it is obtained:

$$\frac{\partial C_i}{\partial t} = D_{ei}\frac{\partial^2 C_i}{\partial z^2} - \frac{\partial (uC_i)}{\partial z} - \frac{1-\varepsilon}{\varepsilon}\rho\frac{\partial q_i}{\partial t} \quad (1)$$

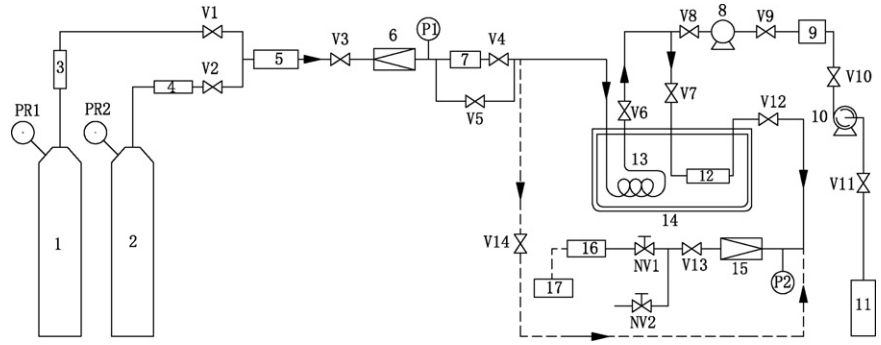

Fig. 2. Schematic flow diagram of the hydrogen isotopes separation apparatus: (1) feed gas, (2) carrier gas, (3 and 4) filter, (5) desiccator, (6) pressure reducing regulator, (7) flow controller, (8) vacuum pump, (9 and 11) gas collector, (10) gas compressor, (12) bed, (13) condensator, (14) liquid nitrogen tank, (15) back pressure regulator, (16) GC, and (17) data analysis system V(1–14) gate valve NV(1–2) needle valve P(1–2) pressure gauge.

The mass balance Eq. (1) describing the concentration distribution along the column accounts for the rate of uptake in the column, the axial dispersion, the convection term and the rate of mass transfer into the particle.

It was proved that the flow rate at the entrance and exit can be considered equal if the concentration of the adsorbed component is less than 20% [15,16]. This assumption is absolutely valid for the present situation where the total content of adsorptive gas is only 7.85%, so the flow rate of the gas is considered as a constant and the variation of u along the adsorbent bed is omitted. Eq. (1) is thus simplified to:

$$\frac{\partial C_i}{\partial t} = D_{ei}\frac{\partial^2 C_i}{\partial z^2} - u\frac{\partial C_i}{\partial z} - \frac{1-\varepsilon}{\varepsilon}\rho\frac{\partial q_i}{\partial t} \tag{2}$$

where $\partial q_i/\partial t$ is the rate of mass transfer into the particle that can be expressed as the linear drive force equation [4,7]:

$$\frac{\partial q_i}{\partial t} = K_i(q_{ei} - q_i) \tag{3}$$

where q_{ei} denotes equilibrium adsorption amount that is calculated by fitting adsorption isotherm of the component i with Langmuir expression (4):

$$q_{ei} = \frac{q_{si}b_iP_i}{(1+b_iP_i)} \tag{4}$$

Over the relevant pressure range, the adsorption isotherms are well represented by the Langmuir expression according to Fig. 3. The fitted values of maximum adsorption amount q_{si} and adsorption affinity b_i are listed in Table 2. For binary components, the adsorption isotherm is described by the extended Langmuir Eq. (5), and the values of q_{si} and b_i are regarded same to the single ones.

$$q_{ei} = \frac{q_{si}b_ip_i}{\left(1+\sum_{i=1}^{n}b_ip_i\right)} = \frac{q_{si}RTb_iC_i}{\left(1+RT\sum_{i=1}^{n}b_iC_i\right)} \tag{5}$$

The boundary condition is:

$$z = 0, \quad \frac{D_{ei}\partial C_i}{\partial z} = -u(C_f - C_i) \tag{6}$$

$$z = L, \quad \frac{\partial C_i}{\partial z} = 0 \tag{7}$$

The initial condition is:

$$t = 0, \quad C_i = 0, \tag{8}$$

Eqs. (2), (3) and (5) together with the initial and boundary conditions constitute the model of the present system. These equations are numerically solved by the finite difference method [4]. Space differential in the model was discretized by the central difference form, then, we can obtain a set of ordinary differential equations that were solved with the Gear method [17]. The values of involved model parameters are listed in Tables 1 and 2.

3.2. Evaluation of model parameters

The overall mass transfer coefficient K_i is given by [18]:

$$\frac{1}{K_i\sigma} = \frac{1}{k_f\sigma} + \frac{1}{k_z\sigma} + \frac{1}{\beta k_s\sigma} \tag{14}$$

where k_f is the mass transfer coefficient that represents the transfer within the boundary layer on the particle surface; k_z is the axial mass transfer coefficient in the packed bed, and βk_s denotes the intraparticle mass transfer coefficient. They are evaluated from the following empirical equations [18,19]:

$$\frac{k_f}{u/\varepsilon}\left(\frac{\mu}{\rho_g D_m}\right)^{2/3} = 1.15\left(\frac{d_p u\rho_g}{\mu\varepsilon}\right)^{-1/2} \tag{15}$$

$$k_z\sigma = \frac{2u}{d_p} \tag{16}$$

$$\beta k_s\sigma = 60(1-\varepsilon_b)\frac{D_i}{d_p^2} \tag{17}$$

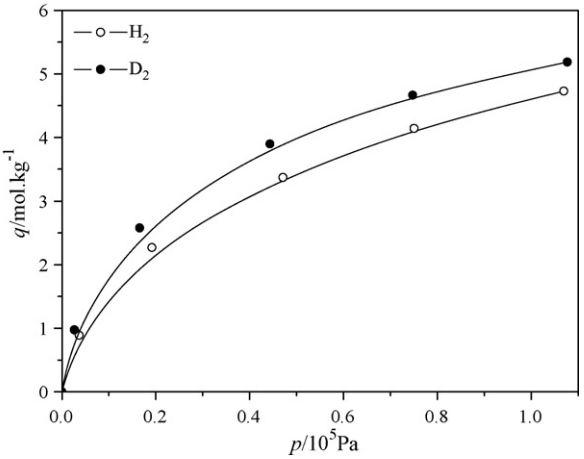

Fig. 3. Adsorption isotherms of H_2 and D_2 at 77 K.

Table 2
Fitted parameters of adsorption isotherms.

Parameter	Hydrogen	Deuterium
q_{si} (mol/kg)	5.94	6.08
b_i (m^3/mol)	3.17	4.55

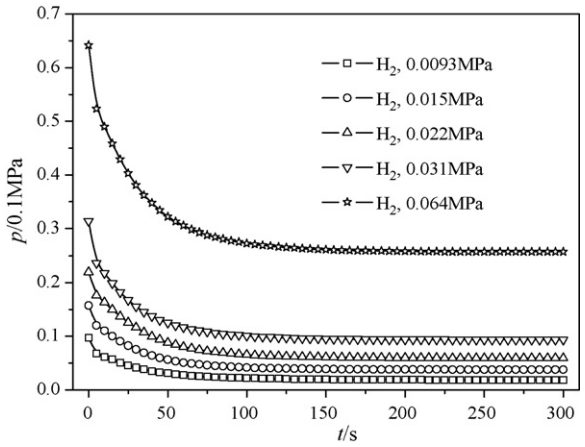

Fig. 4. Dynamic adsorption isotherms of hydrogen at different initial pressures.

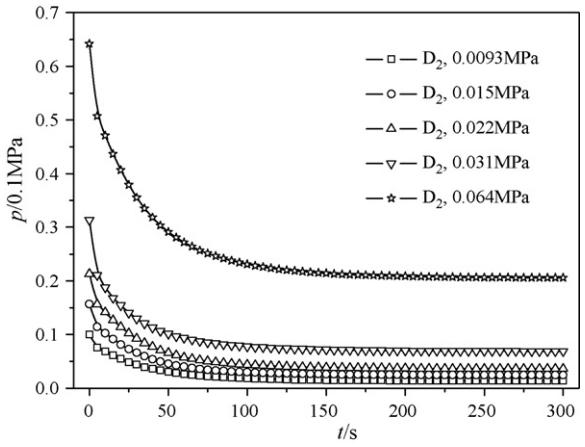

Fig. 5. Dynamic adsorption isotherms of deuterium at different initial pressures.

Assuming the pore diffusion and the surface diffusion in the adsorbent occur simultaneously, D_i, D_{mi} and D_{ei} are estimated by the following empirical equations [20,21]:

$$D_i = \frac{1}{\kappa^2}\varepsilon_p\left(\frac{1}{D_{mi}} + \frac{1}{D_{K_i}}\right)^{-1} + \frac{1}{\kappa^2}\rho_s\frac{dq_i}{dC_i}D_{si} \tag{18}$$

$$D_{mi} = \frac{10^{-5}T^{1.75}(1/M_i + 1/M_{He})^{1/2}}{p[(\sum v_i)^{1/3} + (\sum v_{He})^{1/3}]^2} \tag{19}$$

$$D_{K_i} = \frac{2}{3}\left(\frac{8RT}{\pi M_i}\right)^{1/2}R_p \tag{20}$$

$$D_{ei} = D_{ai}\frac{\varepsilon}{\tau} \tag{21}$$

$$D_{ai} = \frac{2R_p u}{Pe} \tag{22}$$

$$\frac{1}{Pe} = \frac{0.73\varepsilon}{Re\cdot Sc} + \frac{0.5}{1 + 9.49\varepsilon/(Re\cdot Sc)} \tag{23}$$

$$Re = \frac{2R_p u\rho_g}{\mu}, \qquad Sc = \frac{\mu}{\rho_g D_{mi}} \tag{24}$$

4. Results and discussion

4.1. Isotope difference in equilibrium adsorption

Since the difference between H_2 and D_2 in adsorption increases as temperature and pressure decreases [22], adsorption isotherms at low pressure were collected at 77 K with the volumetric method, which are shown in Fig. 3. The ratio of the adsorbed amount of D_2 over H_2 at the given pressure is used as an index of isotope difference in equilibrium adsorption, and the results indicate that the ratios of the adsorption amount of D_2 over H_2 were only 1.18 and 1.17 at 0.0139 and 0.0175 MPa, respectively. Namely, isotope difference in the equilibrium adsorption contributes less to the separation factor.

4.2. Isotope difference in adsorption rate constant

Kinetic adsorption isotherms of H_2 and D_2 on the molecular sieve Y were measured at 77 K with the volumetric method for the five levels of initial pressure, which are shown in Figs. 4 and 5.

The data in Figs. 4 and 5 were dealt with the following model that is expressed as [10]:

$$\ln\left[\frac{(1 - q_t/q_e)}{(1/c - q_t/q_e)}\right] = k(c_2 - c_1)t + C' \tag{25}$$

$$c_1 = \frac{p_1V_1}{V_1 + V_{ad}(T_1/T_2)}, \quad c_2 = \frac{q_eRT_1}{V_1 + V_{ad}(T_1/T_2)}, \quad c = \frac{c_2}{c_1} \tag{26}$$

where P_1, V_1 and T_1 are the initial gas pressure, volume and temperature in the reference cell, V_{ad} and T_2 are the volume and temperature of the adsorption cell. The kinetic data were plotted in $\ln[(1 - q_t/q_e)/(1/c - q_t/q_e)]$ versus t that is shown in Figs. 6 and 7. Based on the slope of straight line, adsorption rate constants were calculated and are listed in Table 3. Here, the isotope difference in adsorption is expressed in the ratio of rate constants of D_2 over H_2, $R_k = k_{D_2}/k_{H_2}$. Two important facts were observed. First, the separation of hydrogen isotopes is of an optimal pressure because the value of R_k increases first and then decreases with the increase of the bulk pressure, moreover, it gives us a revelation that effective separation of hydrogen isotopes should be at the low pressure. Second, the adsorption rate of D_2 is higher than that of H_2 if the pressure is low, which is due to kinetic isotope quantum molecular sieving at low temperature, namely, the zero-point energy of H_2 is larger than that of D_2 at low temperature, therefore, deuterium can be preferentially adsorbed on the adsorbent in the column [23,24]. However, the sequence can be switched over for the condition of higher pressure.

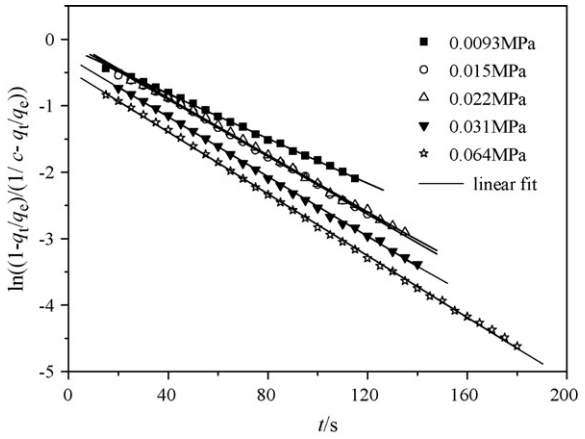

Fig. 6. The plot of $\ln[(1 - q_t/q_e)/(1/c - q_t/q_e)] \sim t$ for H_2.

Table 3
Rate constants of adsorption for the different initial pressure.

Adsorbent/pore size	k MPa^{-1} s^{-1}	0.0093 MPa	0.015 MPa	0.022 MPa	0.031 MPa	0.064 MPa
Y	k_{H_2}	8.23	5.29	3.57	2.37	0.89
0.6–0.7 nm	k_{D_2}	10.60	6.96	4.56	2.55	0.87
	k_{D_2}/k_{H_2}	1.29	1.32	1.28	1.05	0.98

4.3. Breakthrough curves of hydrogen and deuterium

Breakthrough curves were measured with the apparatus in Fig. 2 in order to further study which adsorption difference for hydrogen isotopes was the most important in the process of pressure swing adsorption. Here, separation efficiency is denoted by the separation factor that is expressed as [19]:

$$\alpha_{ij} = \frac{(x/y)_i}{(x/y)_j} \tag{28}$$

where x and y represent molar fraction of the corresponding component in the adsorbed phase and gas phase at equilibrium, respectively. The detailed calculation method was discussed in our previous paper [25].

When length of the packed bed is 1 m and temperature is 77 K, breakthrough curves at the total flow rate 129.79 cm^3/min are shown in Fig. 8 with solid line for the four levels of pressure, and breakthrough curves at the total pressure 0.4 MPa are shown in Fig. 9 with solid line for the four levels of flow rate. Other operation conditions and the corresponding separation factors are listed in Table 4.

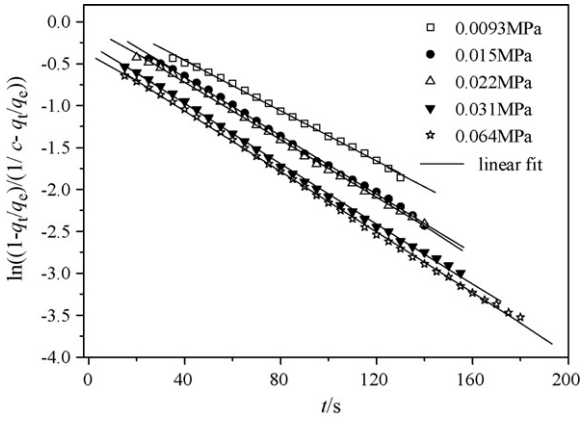

Fig. 7. The plot of $\ln[(1 - q_t/q_e)/(1/c - q_t/q_e)] \sim t$ for D_2.

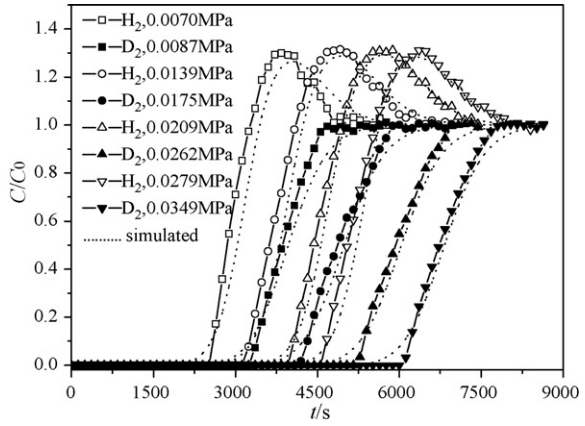

Fig. 8. Experimental and simulated breakthrough curves of H_2 and D_2 gas at different pressures.

The results in Table 4 show that the separation factors increase first and then decrease with the increase of flow rate or pressure, and arrive at maximum value 1.52 at the total gas pressure of 0.4 MPa and flow rate of 129.79 cm^3/min. However, the separation factor is approximately equal at the total pressure of 0.2, 0.4 and 0.6 MPa when other experimental operation conditions are same, therefore, from considering the balance of energy cost and selectivity, 0.2 MPa is selected as the suitable operation pressure. In Figs. 8 and 9, there are profile peaks on H_2 breakthrough curves, say, the exit concentration C/C_0 of hydrogen is larger than 1 before the breakthrough of deuterium from the adsorption bed. It is because the deuterium molecules have higher adsorption rate and adsorption affinity that can displace the adsorbed hydrogen molecules [23,24]. Furthermore, the results indicate that H_2 and D_2 separation on the molecular sieve Y was of good effect due to their steep mass transfer frontal.

Generally speaking, the mechanisms of gas separation based on adsorption are three types: steric effect, equilibrium effect and dynamic effect [7]. First, the separation of hydrogen and deuterium mixture does not rely on the steric effect due to its similarity of molecular size. Second, the equilibrium adsorption difference is very small, which contributes less to this separation process. However, the dynamic selectivity of hydrogen and deuterium in the column is much higher than selectivity of equilibrium adsorption, so the separation of hydrogen and deuterium mainly depends on their dynamic effect in the column. And this dynamic effect is partly embodied in difference of the adsorption rate constants that is due to kinetic isotope quantum molecular sieving, therefore, deuterium can be preferentially adsorbed on the adsorbent [23,24]. Additionally, deuterium molecules diffuse faster in pores of the adsorbent than hydrogen molecules at low temperature when pore size is 0.8 nm or less [24,26], moreover, the quantum spreading of H_2 is wider than that of D_2 at low temperature and pressure [22]. Two reasons above cause the value of D_{ei} and K_i for deuterium larger than that of hydrogen, which also have a little contribution on the dynamic separation.

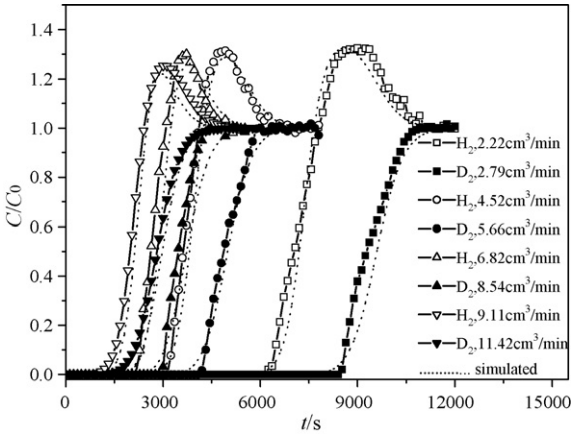

Fig. 9. Experimental and simulated breakthrough curves of H_2 and D_2 gas at different flow rates.

Table 4
Experiment conditions and separation factors.

Total pressure, MPa	Total flow rate, ml/min	Flow rate of H_2, ml/min	Flow rate of D_2, ml/min	Partial pressure of H_2, MPa	Partial pressure of D_2, MPa	Separation factor
0.4	63.75	2.22	2.79	0.0139	0.0175	1.45
0.4	129.79	4.52	5.66	0.0139	0.0175	1.52
0.4	195.76	6.82	8.54	0.0139	0.0175	1.49
0.4	261.62	9.11	11.42	0.0139	0.0175	1.38
0.2	129.79	4.52	5.66	0.0070	0.0087	1.50
0.6	129.79	4.52	5.66	0.0209	0.0262	1.48
0.8	129.79	4.52	5.66	0.0279	0.0349	1.45

4.4. Simulated breakthrough curve

The breakthrough curves of hydrogen and deuterium in Figs. 8 and 9 were simulated by numerically solving the mathematical equations in Section 2 and the involved parameters are given in Tables 1–3 [4]. The dashed smooth curves in Figs. 8 and 9 indicate that the simulation results fit the experimental dots well. Therefore, it is useful not only for discussing the effect of major design or operational variables, but is also applicable in process simulation [27].

5. Conclusions

The two experimental apparatus were designed by us to study behaviors of equilibrium and dynamic adsorption. The results show adsorption rate constants of D_2 are higher than that of H_2 at low pressure, however, the sequence can be switched over for the condition of higher pressure, and the ratio of adsorption rate constants, R_k, increases first and then decreases with the increase of gas pressure. Furthermore, hydrogen isotope gas separation mainly depends on their dynamic difference at low temperature and pressure based on the difference between equilibrium adsorption and dynamic adsorption in the column. In addition, a model proposed for the column can predict the breakthrough curves under different experimental conditions and the simulated breakthrough curves are in good agreement with the experimental ones.

Acknowledgements

The authors are grateful for the financial support of the Natural Science Foundation of Jiangsu Universities (08KJD530002) and the Program for Science and Technology Development of Huai'an (HAG08041).

References

[1] J.B. Zhou, K.S. Wang, L.P. Gao, The purification of hydrogen isotope gas by cryogenic adsorption method, Cryogenics 138 (2004) 50–52.
[2] Z.Y. Guo, Chemistry of Stable Isotopes, 17th ed., Science Press, Beijing, 1984.
[3] H.K. Rae, Separation of Hydrogen Isotopes, American Chemical Society, Washington, DC, 1978.
[4] D.H. Zhang, A. Kodama, M. Goto, et al., Kinetics in hydrogen isotopes cryogenic adsorption, Sep. Purif. Technol. 37 (2004) 1–8.
[5] S. Fukuda, H. Fujiwara, Possibility of separation of deuterium from natural hydrogen by a palladium particle bed, Sep. Sci. Technol. 34 (1999) 2234–2242.
[6] S. Fukuda, K. Fuchinoue, M. Nishigawa, Isotope separation factor and isotopic exchange rate between hydrogen and deuterium of palladium, J. Nucl. Mater. 226 (1995) 311–318.
[7] D.M. Ruthven, S. Farooq, K.S. Knaebel, Pressure Swing Adsorption, VCH Publisher, New York, 1994.
[8] X.Z. Chu, J.M. Xu, Relationship between the adsorption capacity of hydrogen isotopes and specific surface area of adsorbents, Chem. J. Chin. Univ. 29 (2008) 775–778.
[9] X.Z. Chu, Y.P. Zhou, L. Zhou, Analysis of hydrogen isotopes with gas chromatography, Chin. J. Anal. Chem. 34 (2006) 629–632.
[10] X.Z. Chu, Y.P. Zhou, Y.Z. Zhang, et al., Adsorption of hydrogen isotopes on micro- and mesoporous adsorbents with orderly structure, J. Phys. Chem. B 110 (2006) 22596–22600.
[11] S.W. Rutherford, D.D. Do, Adsorption dynamics of carbon dioxide on a carbon molecular sieve 5A, Carbon 38 (2000) 1339–1350.
[12] K.S. Knaebel, F.B. Hill, Pressure swing adsorption: development of an equilibrium theory for gas separations, Chem. Eng. Sci. 40 (1985) 2351–2360.
[13] J.C. Kayser, K.S. Knaebel, Pressure swing adsorption: development of an equilibrium theory for binary gas mixtures with nonlinear isotherms, Chem. Eng. Sci. 44 (1989) 1–8.
[14] G.F. Fernandez, C.N. Kenny, Modeling the pressure swing air separation process, Chem. Eng. Sci. 38 (1983) 827–834.
[15] A. Malek, S. Farooq, Effect of velocity variation due to adsorption–desorption on equilibrium data from breakthrough experiments, Chem. Eng. Sci. 50 (1995) 727–740.
[16] A. Malek, S. Farooq, Determination of equilibrium isotherms using dynamic column breakthrough and constant flow equilibrium desorption, J. Chem. Eng. Data 41 (1996) 25–32.
[17] X.Z. Chu, Studies on the Mechanism and Model of Chemical Oscillations [D], Tianjin University, Tianjin, China, 2004.
[18] M. Nishikawa, K.I. Tanaka, M. Uetake, Mass transfer coefficients in cryosorption of hydrogen isotopes on molecular sieves or activated carbon at 77.4 K, Fusion Technol. 28 (1995) 1738–1748.
[19] D.M. Ruthven, Principles of Adsorption and Adsorption Processes, John Wiley & Sons, New York, 1984.
[20] S.Y. Jia, C.J. Chai, Mass Transfer and Separation Process of Chemical Engineering, Chemical Industry Press, Beijing, China, 2001.
[21] K. Jothimurugesan, D.P. Harrison, Reaction between H_2S and zinc oxide–titanium oxide sorbents. 2. Single-pellet sulfidation modeling, Ind. Eng. Chem. Res. 29 (1990) 1167–1172.
[22] H. Tanaka, H. Kanoh, M. Yudasaka, et al., Quantum effects on hydrogen isotope adsorption on single-walled nanohorns, J. Am. Chem. Soc. 127 (2005) 7511–7516.
[23] A.V. Anil Kumar, S.K. Bhatia, Kinetic molecular sieving of hydrogen isotopes feasible, J. Phys. Chem. C 112 (2008) 11421–11426.
[24] X.B. Zhao, S. Villar-Rodil, A.J. Fletcher, et al., Kinetic isotope effect for H_2 and D_2 quantum molecular sieving in adsorption/desorption on porous carbon materials, J. Phys. Chem. B 110 (2006) 9947–9955.
[25] L. Zhou, W.C. Guo, Y.P. Zhou, A feasibility study of separating CH_4/N_2 by adsorption, Chin. J. Chem. Eng. 10 (2002) 558–561.
[26] L. Tun, E.M. Goldfield, S.K. Gray, Quantum states of molecular hydrogen and its isotopes in single-walled carbon nanotubes, J. Phys. Chem. B 107 (2003) 12989–12995.
[27] X.Z. Chu, Studies on the Adsorption of Hydrogen Isotopes [D], Tianjin University, Tianjin, China, 2007.